crystals

MDPI

Article

New Crystal Forms for Biologically Active Compounds. Part 2: Anastrozole as N-Substituted 1,2,4-Triazole in Halogen Bonding and Lp-π Interactions with 1,4-Diiodotetrafluorobenzene

Mariya A. Kryukova, Alexander V. Sapegin, Alexander S. Novikov, Mikhail Krasavin and Daniil M. Ivanov *

Institute of Chemistry, Saint Petersburg State University, Universitetskaya Nab. 7/9, 199034 Saint Petersburg, Russia; mary_kryukova@mail.ru (M.A.K.); sapegin_yar@mail.ru (A.V.S.); ja2-88@mail.ru (A.S.N.); krasavintm@gmail.com (M.K.)

* Correspondence: st024644@student.spbu.ru

Received: 28 March 2020; Accepted: 2 May 2020; Published: 5 May 2020

Abstract: For an active pharmaceutical ingredient, it is important to stabilize its specific crystal polymorph. If the potential interconversion of various polymorphs is not carefully controlled, it may lead to deterioration of the drug's physicochemical profile and, ultimately, its therapeutic efficacy. The desired polymorph stabilization can be achieved via co-crystallization with appropriate crystallophoric excipients. In this work, we identified an opportunity for co-crystallization of anastrozole (**ASZ**), a well-known aromatase inhibitor useful in second-line therapy of estrogen-dependent breast cancer, with a classical XB donor, 1,2,4,5-tetrafluoro-3,6-diiodobenzene (**1,4-FIB**). In the X-ray structures of **ASZ**·1.5 (**1,4-FIB**) co-crystal, different non-covalent interactions involving hydrogen and halogen atoms were detected and studied by quantum chemical calculations and QTAIM analysis at the ωB97XD/DZP-DKH level of theory.

Keywords: anastrozole; non-covalent interactions; halogen bonding; lp-π interactions; DFT; QTAIM

1. Introduction

The generation of a new salt form is a proven way to modify the physical and chemical properties of an active pharmaceutical ingredient (API) [1]. To be able to give rise to a new salt form, however, the API in question should be ionizable. For non-ionizable APIs, co-crystallization with a crystallophoric excipient (non-API component of the solid drug form) has become an alternative, proven way of accessing a broad range of solid forms and thus modifying various physicochemical properties and increasing API's stability [2–4]. An overwhelming majority of API co-crystals reported today are based on hydrogen bonding as the principal means of constructing the crystalline form. However, halogen bonds have emerged as an equally promising basis for designing new co-crystalline API forms [5–12]. However, despite the emergence of this intriguing supramolecular interaction, halogen-bonded API co-crystals remain relatively scarce. This may have to do with the limited range of pharmaceutically acceptable excipients containing polarized halogen atoms [13]. In continuation of our efforts to identify new crystalline forms for APIs that would be stabilized by halogen bonding [14,15], we turned our attention to screening of crystallization conditions for the title compound, anastrozole (IUPAC name 2,2′-(5-((1H-1,2,4-triazol-1-yl)methyl)-1,3-phenylene)bis(2-methylpropanenitrile), abbreviated as ASZ), which is an aromatase inhibitor useful in second-line therapy of estrogen-dependent breast cancer [16–18].

We choose this API as a potential recipient of XB due to its 1,2,4-triazole moiety, containing at least two nucleophilic $N_{sp}2$ atoms as potential XB acceptor centers. One of them is a hydrogen bond [19] (HB) acceptor in the crystal structure of ASZ itself (Figure 1) [20].

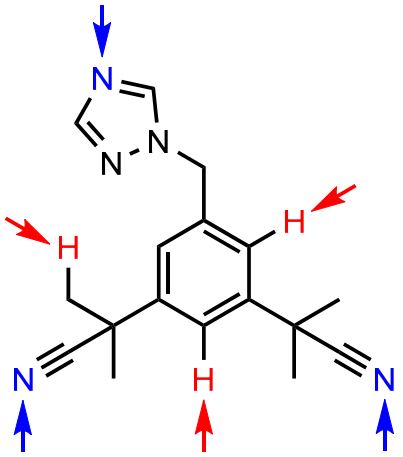

Figure 1. Structure of anastrozole with assigned hydrogen bond donor (red) and hydrogen bond acceptor centers (blue) found in its crystal structure (SATHOL) [20].

Previously, we successfully cocrystallized another API, nevirapine, with classic XB donor, 1,2,4,5-tetrafluoro-3,6-diiodobenzene (also known as 1,4-diiodotetrafluorobenzene, **1,4-FIB**). Noticeably, **1,4-FIB** has already been employed in the co-crystal formation for a number of biologically active compounds including nicotine [21], pyrazinamide, lidocaine, and pentoxifylline [22]. It should be noted, however, that in these studies (as well as in present work), **1,4-FIB** is employed as an exploratory co-crystallization partner. For its use as an excipient for the design of solid drug forms, a further clinical investigation will be required. In this work, we found ASZ can also be cocrystallized with **1,4-FIB** from their solution in MeOH, forming the 2:3 adduct. Herein, we present the results of combined single-crystal XRD experimental and theoretical studies of the adduct and noncovalent interactions found in it.

2. Materials and Methods

2.1. Materials

Anastrozole, 1,2,4,5-tetrafluoro-3,6-diiodobenzene, and MeOH were obtained from a commercial source and used as received.

2.2. X-ray Structure Determination

Crystal of **ASZ**·1.5(**1,4-FIB**) was investigated on an Xcalibur, Eos diffractometer at 100 K (monochromated MoKα radiation with λ = 0.71073 Å). The structure was solved by the direct methods (SHELX program [23]) in the OLEX2 program package [24]. The carbon-bound H atom positions were calculated and included in the refinement in the 'riding' model approximation. U_{iso}(H) were set to 1.5U_{eq}(C) (for CH_3 groups) or 1.2Ueq(C) (for CH_2 and CH groups). The C–H bond lengths are 0.98 Å for CH_3 groups, 0.99 Å for CH_2 groups, and 0.95 Å for CH groups. Empirical absorption correction was applied in the CrysAlisPro [25] program. For crystallographic data and refinement parameters see Supplementary material (Table S3). Supplementary crystallographic data was deposited at Cambridge Crystallographic Data Centre (CCDC 1960975) and can be obtained free of charge via www.ccdc.cam.ac.uk/data_request/cif.

2.3. Powder X-ray Diffraction Experiments

The X-ray diffraction of powder samples was measured at room temperature on a D8 Discover high-resolution diffractometer using monochromated CuKα (λ = 1.54184 Å) radiation.

2.4. Computational Details

The single point calculations based on the experimental X-ray geometry of (**ASZ**)$_3$·(**1,4-FIB**)$_4$ have been carried out at the DFT level of theory using the dispersion-corrected hybrid functional ωB97XD [26] with the help of the Gaussian-09 [27] program package. The Douglas–Kroll–Hess 2nd order scalar relativistic calculations requested relativistic core Hamiltonian were carried out using the DZP-DKH basis sets [28–31] for all atoms. The topological analysis of the electron density distribution with the help of the atoms in molecules (QTAIM) method developed by Bader [32] has been performed by using the Multiwfn program [33]. The Cartesian atomic coordinates of a model supramolecular cluster are presented in Supporting Information, Table S4.

3. Results and Discussion

*3.1. Halogen Bonding in **ASZ**·1.5(**1,4-FIB**)*

Slow evaporation of a MeOH solution of **ASZ** with **1,4-FIB** taken in a 1:1 ratio leads to the formation on single crystals of **ASZ**·1.5(**1,4-FIB**) suitable for the X-ray diffraction experiment. It is notable that we also tried to synthesize the **ASZ**·1.5(**1,4-FIB**) pure phase both by mechanical grinding of 2:3 **ASZ** + **1,4-FIB** mixture with MeOH additions during the process or by crystallization of the same 2:3 mixture from methanol with the following grinding of obtained crystalline material. Powder X-ray diffraction experiments for both cases show that **ASZ**·1.5(**1,4-FIB**) coexists with some other unidentified phases (see Figures S3 and S4 in SI). For details on the powder x-ray diffraction experiments see also Section 2.3.

According to the single-crystal XRD data, the cocrystallization of **ASZ** with **1,4-FIB** does not lead to any relevant changes, considering the 3σ criterion, in covalent bond lengths of **ASZ** [20] and **1,4-FIB** [34].

As expected, the C–I···N contacts were found in **ASZ**·1.5(**1,4-FIB**) (Figure 2), which can be interpreted as halogen bonding [35]. In accordance with their geometrical parameters (Table 1), the theoretically estimated energies of these contacts are 4.6–5.3 kcal/mol (I3S···N2) and 4.8–6.0 kcal/mol (I1S···N3), which is comparable with a lower limit for strength of "moderate" hydrogen bonding according to Jeffrey's classification ("strong": 40−15 kcal/mol; "moderate": 15−4 kcal/mol; "weak": <4 kcal/mol) [36]. For **1,4-FIB**, the molecular electrostatic potential calculations were reported [37–39], which confirm the σ-hole electrophilicity [40,41] of iodine atoms in this molecule.

Table 1. Parameters of the C–I···X XBs in **ASZ**·1.5(**1,4-FIB**).

C–I···X	*d*(I···X), Å	R_{IX} [b]	∠(C–I···X),°
C8S–I3S···N2	2.913 (6)	0.83	175.3 (2)
C1S–I1S···N3	2.883 (7)	0.82	169.3 (2)
C4S–I2S···F6S	3.390 (5)	0.98	149.97 (19)
C4S–I2S···I3S	3.8529 (8)	0.97	157.68 (18)
Comparison [a]	*3.53 (I···N)* *3.45 (I···F)* *3.96 (I···I)*	*1.00*	*180*

[a] Comparison is the vdW radii sum [42] for distances and classic XB angle. [b] $R_{IX} = d(I\cdots X)/(R_{vdW}(I) + R_{vdW}(X))$.

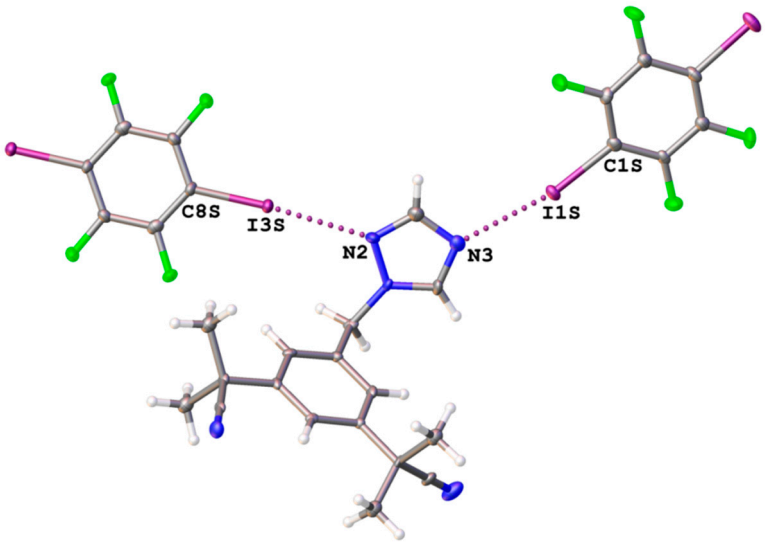

Figure 2. The C–I···N XBs in anastrozole **(ASZ)**·1.5(**1,4-FIB**). Hereinafter noncovalent interactions were assigned by dotted lines and ellipsoids are drawn with 50% probability.

Previously, the C–I···N XBs including 1,2,4-triazole moiety was mentioned only in two metal-organic frameworks (FALNEN [43] and UMOTOG [44]) and one free 4*H*-1,2,4-triazole (FARCIN01 [45]). We analyzed all the structures containing the C–I···N XBs with 1,2,4-triazoles in CCDC and found 9 more structures [44,46–52]. It is notable that in all corresponding works, these interactions were not even mentioned. The I···N distances are in the range of 2.839 (4)–3.378 (3) Å, and the ∠(C–I···N) angles vary from 157.18 (17) to 177.57 (8)° (for details see Table S1 in supplementary materials). In **ASZ**·1.5 (**1,4-FIB**), both distances (2.883 (7) and 2.913 (6) Å) are shorter than in most previously published structures, which can be explained by the electron-withdrawing I substituent in **1,4-FIB**. Noticeably, the C–Cl···N [53–55] and C–Br···N [45,53,56–58] XBs including 1,2,4-triazole moiety are also mentioned in the literature.

Halogen bonding was also found between **1,4-FIB** molecules, represented by bifurcated C–I···(I,F) contact (Figure 3). Both distances are less than vdW sums, and both angles are around 150° (Table 1) and fall into an acceptable value for XBs. These non-covalent interactions are weak, viz. 1.3 kcal/mol in the case of I2S···F6S and 1.6 kcal/mol in the case of I2S···I3S.

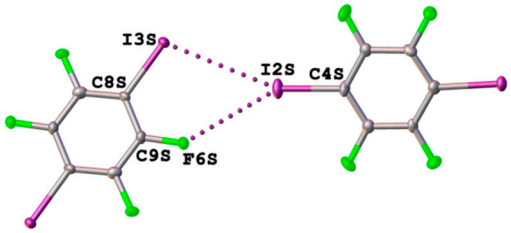

Figure 3. Bifurcated C–I···(I,F) halogen bonding between **1,4-FIB** molecules in **ASZ**·1.5(**1,4-FIB**).

A resembling feature can be found in the structure KUWRAX [59], where both I···F and I···I distances are less than the corresponding vdW sums (3.6889 (7) vs 3.96 Å and 3.409 (3) vs 3.45 Å), however, in this structure, the corresponding ∠(C–I···F) angle (125.09 (13)°) is not high enough to recognize this interaction as halogen bonding. Thus, **ASZ**·1.5(**1,4-FIB**) demonstrates the first example of bifurcated C–I···(I,F) halogen bonding between **1,4-FIB** molecules.

*3.2. Lone-Pair···π Interactions in **ASZ**·1.5(**1,4-FIB**)*

Besides the expected C–I···N halogen bonding, the C···I–C contacts (Table 2) were identified between **ASZ** and **1,4-FIB** molecules in **ASZ**·1.5 (**1,4-FIB**) (Figure 4). According to the ∠(C···I–C) angle, which is close to 90° (Table 2), this interaction can be interpreted as lp(I)···π(C) interaction [60]. Their theoretically estimated strength is 1.6 kcal/mol.

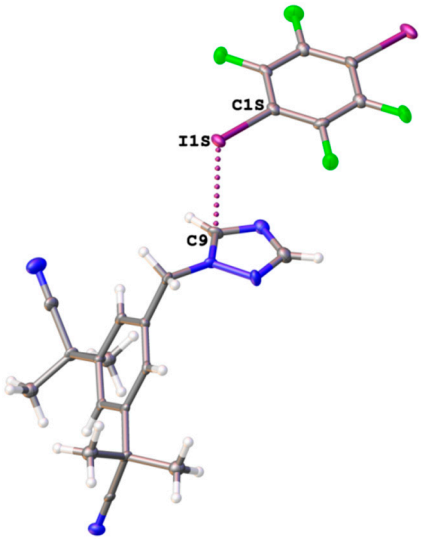

Figure 4. The lp(I)···π(C) interaction between **ASZ** and **1,4-FIB** molecules in **ASZ**·1.5(**1,4-FIB**).

Table 2. Parameters of the lp(I)···π(C) interactions in **ASZ**·1.5(**1,4-FIB**).

C···I–C	*d*(C···I), Å	R_{CI} [b]	∠(C···I–C),°
C9···I1S–C1S	3.528 (8)	0.96	86.6(3)
C9S···I2S–C4S	3.686 (8)	1.00	92.9(3)
Comparison [a]	*3.68*	*1.00*	*90*

[a] Comparison is the vdW radii sum [42] for distances and classic XB acceptor angle. [b] $R_{CI} = d(C\cdots I)/(R_{vdW}(I) + R_{vdW}(C))$.

Previously, the lp(I)···π(C) interactions including 1,2,4-triazole moiety were discussed only for five 1,2,4-triazolium iodides [61,62], where these interactions are interionic. We analyzed the CCDC data and identified 23 more structures with the C···I interactions including 1,2,4-triazoles. 1,2,4-triazolium iodides [20,63–70] were also found in 15 structures. The C···I–M interactions [71–76] in 1,2,4-triazole-containing MOFs were detected in 6 structures. Structure XIWGOC contains the C···I^- interactions between the cationic Ir^{III} complex and iodide counterion [77]. Only in the IDIFEH structure was another example of the C···I–C interactions between neutral isolated molecules [78] identified. The C···I distances vary from 3.4363(2) to 3.670 (3) Å (for details see Table S2), and the C9···I1S distance (3.528 (8) Å) in **ASZ**·1.5(**1,4-FIB**) is within this range.

Besides, possible lp(I)···π(C) interaction between **1,4-FIB** molecules was found (Figure 5). Although the C···I distance is around the vdW sum (3.686 (8) vs 3.68 Å), further theoretical calculations performed on experimentally determined atomic coordinates (see next section) confirmed the existence of the interaction and its noncovalent nature (estimated energy is 0.9–1.1 kcal/mol). Notably, the same interactions were found by us for **1,4-FIB** and other iodofluorobenzenes [60,79,80].

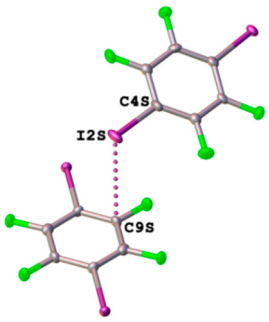

Figure 5. The lp(I)···π(C) interaction between **1,4-FIB** molecules in **ASZ**·1.5(**1,4-FIB**).

*3.3. Hydrogen Bonding in **ASZ**·1.5(**1,4-FIB**)*

As well as in the structure of free **ASZ**, cyano N atoms are involved in weak hydrogen bonding (theoretically estimated strength of appropriate contacts vary from 0.9 to 1.9 kcal/mol) (Figure 6 and Table 3). Apart from methyl H atoms, the hydrogen atom in the methylene group is also an HB donor, which was not observed in the **ASZ** structure previously.

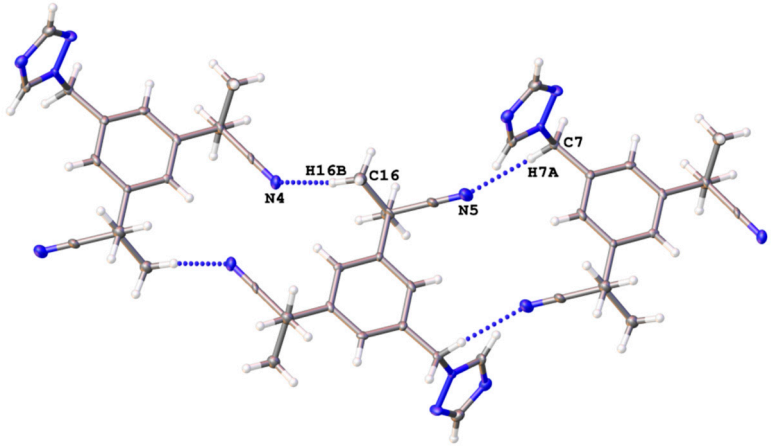

Figure 6. The C–H···N HBs in **ASZ**·1.5(**1,4-FIB**).

Table 3. Parameters of the C–H···N HBs in **ASZ**·1.5(**1,4-FIB**).

C–H···N	*d*(H···N), Å	R_{HN} [b]	*d*(C···N), Å	∠(C–I···X),°
C7–H7A···N5	2.484	0.90	3.441 (10)	168.6
C16–H16B···N4	2.733	0.99	3.62 (1)	153.9
Comparison [a]	*2.75*	*1.00*	*3.25*	*110.0*

[a] Comparison is the vdW radii sum [42] for distances and minimal HB angle. [b] R_{HN} = *d*(H···N)/(R_{vdW}(H) + R_{vdW}(N)).

*3.4. Theoretical Study of Different Non-covalent Interactions in **ASZ**·1.5(**1,4-FIB**)*

The supramolecular structure of **ASZ**·1.5(**1,4-FIB**) is formed by various non-covalent contacts (viz. lp-π interactions, hydrogen, and halogen bonding). We performed quantum chemical calculations and QTAIM analysis [32] to study the nature and energies of these non-covalent contacts in a model supramolecular cluster (**ASZ**)$_3$·(**1,4-FIB**)$_4$ based on the appropriate X-ray diffraction data (Supporting Information, Table S4). This approach depends very slightly on the basis set [81,82] or method [83,84] used and it was already successfully used by us previously for similar chemical systems [14,15,79,85,86] and upon studies of different non-covalent interactions (e.g., hydrogen/chalcogen/halogen bonds, stacking interactions, metallophilic interactions) in other organic and inorganic compounds [14,15,87–92]. The results of QTAIM analysis are presented in Table 4 and visualized in Figure 7.

Table 4. Values of the density of all electrons—ρ(**r**), Laplacian of electron density—$\nabla^2\rho(\mathbf{r})$, energy density—H_b, potential energy density—V(**r**), and Lagrangian kinetic energy—G(**r**) (a.u.) at the bond critical points (3, −1), corresponding to different non-covalent interactions in (**ASZ**)$_3$·(**1,4-FIB**)$_4$, bond lengths—*l* (Å), as well as energies for these contacts E_{int} (kcal/mol), defined by two approaches.*·

Contact	ρ(r)	∇2ρ(r)	Hb	V(r)	G(r)	Einta	Eintb	*l*
I3S···N2	0.022	0.070	0.000	−0.017	0.017	5.3	4.6	2.913
I1S···N3	0.024	0.072	0.000	−0.019	0.018	6.0	4.8	2.883
I2S···F6S	0.006	0.026	0.001	−0.004	0.005	1.3	1.3	3.390
I2S···I3S	0.008	0.031	0.001	−0.005	0.006	1.6	1.6	3.853
C9···I1S	0.009	0.029	0.001	−0.005	0.006	1.6	1.6	3.528
C9S···I2S	0.006	0.023	0.001	−0.003	0.004	0.9	1.1	3.686
H7A···N5	0.009	0.033	0.001	−0.006	0.007	1.9	1.9	2.484
H16B···N4	0.005	0.021	0.001	−0.003	0.004	0.9	1.1	2.733

[a] $E_{int} = -V(\mathbf{r})/2$ [93] [b] $E_{int} = 0.429G(\mathbf{r})$ [94] * Note that Tsirelson et al. [95] also proposed alternative correlations developed exclusively for non-covalent interactions involving iodine atoms, viz. $E_{int} = 0.68(-V(\mathbf{r}))$ or $E_{int} = 0.67G(\mathbf{r})$.

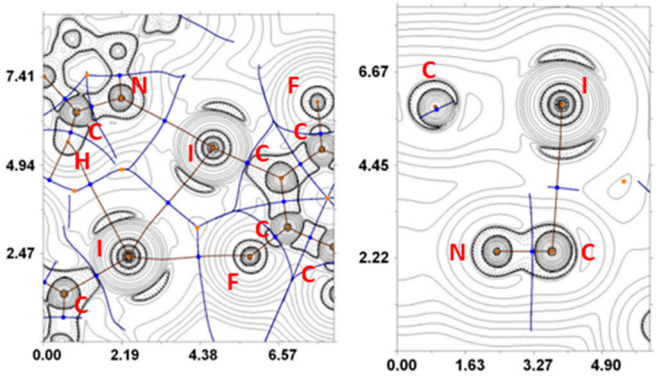

Figure 7. Contour line diagrams of the Laplacian distribution $\nabla^2\rho(\mathbf{r})$, bond paths and selected zero-flux surfaces referring to the C–I···X (X = N, F, I) halogen bonding (left) and lp(I)···π(triazole) (right) interactions in (**ASZ**)$_3$·(**1,4-FIB**)$_4$. Bond critical points (3, −1) are shown in blue, nuclear critical points (3, −3) in pale brown, ring critical points (3, +1) in orange, cage critical points (3, +3) in light green. Length units—Å.

The QTAIM analysis reveals the existence of bond critical points (3, −1) (BCPs) for all non-covalent interactions listed in Table 4. The properties of electron density, Laplacian of electron density and energy density in these BCPs are common for non-covalent interactions. Energies for these non-covalent contacts (vary from 0.9 to 6.0 kcal/mol) were defined according to the procedures developed by Espinosa et al. [93] and Vener et al. [94] using the equations $E_{int} = 0.5(-V(\mathbf{r}))$ or $E_{int} = 0.429G(r)$, respectively. The balance between the potential energy density V(**r**) and Lagrangian kinetic energy G(**r**) at the BCPs reveals that a covalent contribution is absent in all supramolecular contacts listed in Table 4, except I1S···N3 halogen bonding [96].

4. Conclusions

In combination with 1,2,4,5-tetrafluoro-3,6-diiodobenzene, a classical XB donor, we have identified a new halogen-bonded solid for anastrozole, an anticancer aromatase inhibitor drug. These findings continue to provide proof-of-principle for the productive employment of halogen bonds in the design and discovery of stable crystalline forms of important drug substances. Moreover, these results suggest that the range of potential XB donors for co-crystallization with basic nitrogen-rich molecular frameworks can potentially be expanded beyond the classical ones. The distinctive features of the crystal structures obtained and characterized in detail in this work are the presence of XBs with both triazole N atoms, firstly found for anastrazole. Apart from that, the adduct structure demonstrates the lp(I)···π(triazole) attractive interactions, which may also be important for the adduct

formation. The findings encourage us to continue searching for yet novel opportunities to detect XBs as indispensable forces leading to the formation of a new crystal. The results of these studies will be reported in due course.

Supplementary Materials: The following are available online at http://www.mdpi.com/2073-4352/10/5/371/s1, Figure S1: Structural motifs around the C–I···N XBs including 1,2,4-triazole moiety in CCDC structures; Figure S2: Structural motifs around the lp(I)···C interactions including 1,2,4-triazole moiety in CCDC structures; Figure S3: Powder X-ray diffraction data (blue line) of mixture, obtained by mechanical grinding of 2**ASZ** + 3(**1,4-FIB**) mixture with MeOH additions; Figure S4: Powder X-ray diffraction data (blue line) of mixture, obtained by grinding of crystalline material grown from 2**ASZ** + 3(**1,4-FIB**) solution in methanol; Table S1: Parameters of the C–I···N XBs including 1,2,4-triazole moiety in CCDC structures; Table S2: Parameters of the lp(I)···C interactions including 1,2,4-triazole moiety in CCDC structures; Table S3: Crystal data and structure refinement for **ASZ**·1.5(**1,4-FIB**); Table S4: Cartesian atomic coordinates of model supramolecular cluster.

Author Contributions: Conceptualization, M.K., A.V.S., and D.M.I.; data curation, D.M.I.; formal analysis, A.S.N. and D.M.I.; funding acquisition, A.V.S.; investigation, M.A.K.; methodology, D.M.I.; project administration, D.M.I.; resources, A.V.S.; software, A.S.N.; supervision, M.K. and D.M.I.; validation, M.A.K.; visualization, A.S.N. and D.M.I.; writing—original draft, A.S.N. and D.M.I.; writing—review & editing, M.K. All authors have read and agreed to the published version of the manuscript.

Funding: This work was funded by Russian Science Foundation, grant number 17-73-20185.

Acknowledgments: Physicochemical studies were performed at the Center for X-ray Diffraction Studies belonging to Saint Petersburg State University.

Conflicts of Interest: The authors declare no conflict of interest.

References

1. Stahl, P.H.; Wermiuth, C.G.E. *Handbook of Pharmaceutical Salts Properties, Selection and Use*; Verlag Helvetica Chimica Acta: Zürich, Switzerland, 2002.
2. Trask, A.V. An overview of pharmaceutical cocrystals as intellectual property. *Mol. Pharm.* **2007**, *4*, 301–309. [CrossRef] [PubMed]
3. Trask, A.V.; Motherwell, W.D.S.; Jones, W. Pharmaceutical cocrystallization: Engineering a remedy for caffeine hydration. *Cryst. Growth Des.* **2005**, *5*, 1013–1021. [CrossRef]
4. Karki, S.; Friščić, T.; Jones, W.; Motherwell, W.D.S. Screening for pharmaceutical cocrystal hydrates via neat and liquid-assisted grinding. *Mol. Pharm.* **2007**, *4*, 347–354. [CrossRef] [PubMed]
5. Merkens, C.; Pan, F.F.; Englert, U. 3-(4-Pyridyl)-2,4-pentanedione—A bridge between coordinative, halogen, and hydrogen bonds. *CrystEngComm* **2013**, *15*, 8153–8158. [CrossRef]
6. Cinčić, D.; Friščić, T.; Jones, W. Structural Equivalence of Br and I Halogen Bonds: A Route to Isostructural Materials with Controllable Properties. *Chem. Mater.* **2008**, *20*, 6623–6626. [CrossRef]
7. Cinčić, D.; Friščić, T.; Jones, W. A cocrystallisation-based strategy to construct isostructural solids. *New J. Chem.* **2008**, *32*, 1776–1781. [CrossRef]
8. Bushuyev, O.S.; Tan, D.; Barrett, C.J.; Friščić, T. Fluorinated azobenzenes with highly strained geometries for halogen bond-driven self-assembly in the solid state. *CrystEngComm* **2015**, *17*, 73–80. [CrossRef]
9. Cinčić, D.; Friščić, T. Synthesis of an extended halogen-bonded metal-organic structure in a one-pot mechanochemical reaction that combines covalent bonding, coordination chemistry and supramolecular synthesis. *CrystEngComm* **2014**, *16*, 10169–10172. [CrossRef]
10. Troff, R.W.; Makela, T.; Topic, F.; Valkonen, A.; Raatikainen, K.; Rissanen, K. Alternative Motifs for Halogen Bonding. *Eur. J. Org. Chem.* **2013**, *2013*, 1617–1637. [CrossRef]
11. Cinčić, D.; Friščić, T.; Jones, W. A stepwise mechanism for the mechanochemical synthesis of halogen-bonded cocrystal architectures. *J. Am. Chem. Soc.* **2008**, *130*, 7524–7525. [CrossRef]
12. Carletta, A.; Spinelli, F.; d'Agostino, S.; Ventura, B.; Chierotti, M.R.; Gobetto, R.; Wouters, J.; Grepioni, F. Halogen-Bond Effects on the Thermo- and Photochromic Behaviour of Anil-Based Molecular Co-crystals. *Chem.: Eur. J.* **2017**, *23*, 5317–5329. [CrossRef] [PubMed]
13. Stilinović, V.; Horvat, G.; Hrenar, T.; Nemec, V.; Cinčić, D. Halogen and Hydrogen Bonding between (N-Halogeno)-succinimides and Pyridine Derivatives in Solution, the Solid State and In Silico. *Chem. Eur. J.* **2017**, *23*, 5244–5257. [CrossRef] [PubMed]

14. Kryukova, M.A.; Sapegin, A.V.; Novikov, A.S.; Krasavin, M.; Ivanov, D.M. New Crystal Forms for Biologically Active Compounds. Part 1: Noncovalent Interactions in Adducts of Nevirapine with XB Donors. *Crystals* **2019**, *9*, 71. [CrossRef]
15. Kryukova, M.A.; Sapegin, A.V.; Novikov, A.S.; Krasavin, M.; Ivanov, D.M. Non-covalent interactions observed in nevirapinium pentaiodide hydrate which include the rare I_4–$I^- \cdots$O=C halogen bonding. *Z. Kristallogr. Cryst. Mater.* **2019**, *234*, 101–108. [CrossRef]
16. Wiseman, L.R.; Adkins, J.C. Anastrozole—A review of its use in the management of postmenopausal women with advanced breast cancer. *Drugs Aging* **1998**, *13*, 321–332. [CrossRef] [PubMed]
17. Augusto, T.V.; Correia-da-Silva, G.; Rodrigues, C.M.P.; Teixeira, N.; Amaral, C. Acquired resistance to aromatase inhibitors: Where we stand! *Endocr.-Relat. Cancer* **2018**, *25*, R283–R301. [CrossRef]
18. Rodgers, R.J.; Reid, G.D.; Koch, J.; Deans, R.; Ledger, W.L.; Friedlander, M.; Gilchrist, R.B.; Walters, K.A.; Abbott, J.A. The safety and efficacy of controlled ovarian hyperstimulation for fertility preservation in women with early breast cancer: A systematic review. *Hum. Reprod.* **2017**, *32*, 1033–1045. [CrossRef]
19. Arunan, E.; Desiraju, G.R.; Klein, R.A.; Sadlej, J.; Scheiner, S.; Alkorta, I.; Clary, D.C.; Crabtree, R.H.; Dannenberg, J.J.; Hobza, P.; et al. Definition of the hydrogen bond (IUPAC Recommendations 2011). *Pure Appl. Chem.* **2011**, *83*, 1637–1641. [CrossRef]
20. Tang, G.P.; Gu, J.M. 2-[3-(2-cyano-2-propyl)-5-(1,2,4-triazol-1-yl)phenyl]-2-methylpropiononitrile. *Acta Cryst. E* **2005**, *61*, O2330–O2331. [CrossRef]
21. Capucci, D.; Balestri, D.; Mazzeo, P.P.; Pelagatti, P.; Rubini, K.; Bacchi, A. Liquid Nicotine Tamed in Solid Forms by Cocrystallization. *Cryst. Growth Des.* **2017**, *17*, 4958–4964. [CrossRef]
22. Choquesillo-Lazarte, D.; Nemec, V.; Cinčić, D. Halogen bonded cocrystals of active pharmaceutical ingredients: Pyrazinamide, lidocaine and pentoxifylline in combination with haloperfluorinated compounds. *CrystEngComm* **2017**, *19*, 5293–5299. [CrossRef]
23. Sheldrick, G. SHELXT - Integrated space-group and crystal-structure determination. *Acta Cryst. A* **2015**, *71*, 3–8. [CrossRef] [PubMed]
24. Dolomanov, O.V.; Bourhis, L.J.; Gildea, R.J.; Howard, J.A.K.; Puschmann, H. OLEX2: A complete structure solution, refinement and analysis program. *J. Appl. Cryst.* **2009**, *42*, 339–341. [CrossRef]
25. Agilent Technologies Ltd. *CrysAlisPro*; Version 1.171.136.120 (release 127-106-2012); Agilent Technologies Ltd.: Santa Clara, CA, USA, 2012.
26. Chai, J.D.; Head-Gordon, M. Long-range corrected hybrid density functionals with damped atom-atom dispersion corrections. *Phys. Chem. Chem. Phys.* **2008**, *10*, 6615–6620. [CrossRef] [PubMed]
27. Frisch, M.J.; Trucks, G.W.; Schlegel, H.B.; Scuseria, G.E.; Robb, M.A.; Cheeseman, J.R.; Scalmani, G.; Barone, V.; Mennucci, B.; Petersson, G.A.; et al. *Gaussian 09, EM64L-G09RevB. 01*; Gaussian, Inc.: Wallingford, CT, USA, 2010.
28. Barros, C.L.; de Oliveira, P.J.P.; Jorge, F.E.; Canal Neto, A.; Campos, M. Gaussian basis set of double zeta quality for atoms Rb through Xe: Application in non-relativistic and relativistic calculations of atomic and molecular properties. *Mol. Phys.* **2010**, *108*, 1965–1972. [CrossRef]
29. de Berrêdo, R.C.; Jorge, F.E. All-electron double zeta basis sets for platinum: Estimating scalar relativistic effects on platinum(II) anticancer drugs. *J. Mol. Struct. THEOCHEM* **2010**, *961*, 107–112. [CrossRef]
30. Jorge, F.E.; Canal Neto, A.; Camiletti, G.G.; Machado, S.F. Contracted Gaussian basis sets for Douglas–Kroll–Hess calculations: Estimating scalar relativistic effects of some atomic and molecular properties. *J. Chem. Phys.* **2009**, *130*, 064108. [CrossRef]
31. Neto, A.C.; Jorge, F.E. All-electron double zeta basis sets for the most fifth-row atoms: Application in DFT spectroscopic constant calculations. *Chem. Phys. Lett.* **2013**, *582*, 158–162. [CrossRef]
32. Bader, R.F.W. A quantum theory of molecular structure and its applications. *Chem. Rev.* **1991**, *91*, 893–928. [CrossRef]
33. Lu, T.; Chen, F. Multiwfn: A multifunctional wavefunction analyzer. *J. Comput. Chem.* **2012**, *33*, 580–592. [CrossRef]
34. Oh, S.Y.; Nickels, C.W.; Garcia, F.; Jones, W.; Friščić, T. Switching between halogen- and hydrogen-bonding in stoichiometric variations of a cocrystal of a phosphine oxide. *CrystEngComm* **2012**, *14*, 6110–6114. [CrossRef]
35. Desiraju, G.R.; Ho, P.S.; Kloo, L.; Legon, A.C.; Marquardt, R.; Metrangolo, P.; Politzer, P.; Resnati, G.; Rissanen, K. Definition of the halogen bond (IUPAC Recommendations 2013). *Pure Appl. Chem.* **2013**, *85*, 1711–1713. [CrossRef]

36. Steiner, T. The hydrogen bond in the solid state. *Angew. Chem.-Int. Ed.* **2002**, *41*, 48–76. [CrossRef]
37. Pandiyan, B.V.; Deepa, P.; Kolandaivel, P. How do halogen bonds (S–O···I, N–O···I and C–O···I) and halogen-halogen contacts (C–I···I–C, C–F···F–C) subsist in crystal structures? A quantum chemical insight. *J. Mol. Model.* **2017**, *23*, 16. [CrossRef]
38. Li, L.L.; Liu, Z.F.; Wu, W.X.; Jin, W.J. Cocrystals with tunable luminescence colour self-assembled by a predictable method. *Acta Crystallogr. Sect. B* **2018**, *74*, 610–617. [CrossRef]
39. DeHaven, B.A.; Chen, A.L.; Shimizu, E.A.; Salpage, S.R.; Smith, M.D.; Shimizu, L.S. Synergistic effects of hydrogen and halogen bonding in co-crystals of dipyridylureas and diiodotetrafluorobenzenes. *Supramol. Chem.* **2018**, *30*, 315–327. [CrossRef]
40. Politzer, P.; Murray, J.S.; Clark, T. Halogen bonding and other s-hole interactions: A perspective. *Phys. Chem. Chem. Phys.* **2013**, *15*, 11178–11189. [CrossRef]
41. Murray, J.S.; Politzer, P. Interaction and Polarization Energy Relationships in s-Hole and p-Hole Bonding. *Crystals* **2020**, *10*, 76. [CrossRef]
42. Bondi, A. Van der Waals volumes + radii. *J. Phys. Chem.* **1964**, *68*, 441–451. [CrossRef]
43. Zhang, K.L.; Hou, C.T.; Song, J.J.; Deng, Y.; Li, L.; Ng, S.W.; Diao, G.W. Temperature and auxiliary ligand-controlled supramolecular assembly in a series of Zn(II)-organic frameworks: Syntheses, structures and properties. *CrystEngComm* **2012**, *14*, 590–600. [CrossRef]
44. Zhang, K.L.; Chang, Y.; Ng, S.W. Preparation and characterization of two supramolecular complexes with 5-amino-2,4,6-triiodoisophthalic acid under N-donor auxiliary ligand intervention. *Inorg. Chim. Acta* **2011**, *368*, 49–57. [CrossRef]
45. Wang, J.W.; Chen, C.; Li, Y.J.; Luo, Y.H.; Sun, B.W. Halogen-bonding contacts determining the crystal structure and fluorescence properties of organic salts. *New J. Chem.* **2017**, *41*, 9444–9452. [CrossRef]
46. Rode, N.D.; Sonawane, A.D.; Garud, D.R.; Joshi, R.R.; Joshi, R.A.; Likhite, A.P. First regioselective iodocyclization reaction of 3-aryl-5-(prop-2-ynylthio)-1H-1,2,4-triazoles. *Tetrahedron Lett.* **2015**, *56*, 5140–5144. [CrossRef]
47. Luo, Y.H.; Sun, Y.; Liu, Q.L.; Yang, L.J.; Wen, G.J.; Wang, M.X.; Sun, B.W. Influence of Halogen Atoms on Spin-Crossover Properties of 1,2,4-Triazole-Based 1D Iron(II) Polymers. *ChemistrySelect* **2016**, *1*, 3879–3884. [CrossRef]
48. Xiong, H.-P.; Gao, S.-H.; Li, C.-T.; Wu, Z.-J. (2*RS*)-2-(2,4-Difluorophenyl)-1-[(4-iodobenzyl)(methyl)amino]-3-(1H-1,2,4-triazol-1-yl)propan-2-ol. *Acta Cryst. E* **2012**, *68*, o2447–o2448. [CrossRef]
49. Li, L.; Chi, Y.; Mang, X.Y.; Zhang, G.Q.; Zhang, Y.; Zhao, T.X.; Huang, M.; Li, H.B. Synthesis, crystal structure and thermal analysis of tetraiodo-4,4′-bi-1,2,4-triazole. *Chin. Chem. Lett.* **2013**, *24*, 786–788. [CrossRef]
50. Il'inykh, E.S.; Kim, D.G.; Kodess, M.I.; Matochkina, E.G.; Slepukhin, P.A. Synthesis of novel fluorine- and iodine-containing [1,2,4]triazolo[3, 4-b][1,3]thiazines based 3-(alkenylthio)-5-(trifluoromethyl)-4H-1,2,4-triazole-3-thiols. *J. Fluorine Chem.* **2013**, *149*, 24–29. [CrossRef]
51. Song, J.; Wu, Z.H.; Wangtrakuldee, B.; Choi, S.R.; Zha, Z.H.; Ploessl, K.; Mach, R.H.; Kung, H. 4-(((4-Iodophenyl)methyl)-4H-1,2,4-triazol-4-ylamino)-benzonitrile: A Potential Imaging Agent for Aromatase. *J. Med. Chem.* **2016**, *59*, 9370–9380. [CrossRef]
52. Nagaradja, E.; Bentabed-Ababsa, G.; Scalabrini, M.; Chevallier, F.; Philippot, S.; Fontanay, S.; Duval, R.E.; Halauko, Y.S.; Ivashkevich, O.A.; Matulis, V.E.; et al. Deprotometalation-iodolysis and computed CH acidity of 1,2,3-and 1,2,4-triazoles. Application to the synthesis of resveratrol analogues. *Bioorg. Med. Chem.* **2015**, *23*, 6355–6363. [CrossRef]
53. Dong, Z.; Zhao, T.X.; Li, L.; Zhang, L.J.; Liang, D.H.; Li, H.B. Synthesis and X-Ray Crystal Structures of Tetrahalogeno-4,4′-bi-1,2,4-triazoles. *Mol. Cryst. Liq. Cryst.* **2015**, *623*, 333–342. [CrossRef]
54. Al-Salahi, R.; Al-Omar, M.; Marzouk, M.; Ng, S.W. 5-Chloro-2-methylsulfonyl-1,2,4-triazolo[1,5-a]quinazoline. *Acta Cryst. E* **2012**, *68*, o1809. [CrossRef] [PubMed]
55. Khan, I.; Panini, P.; Khan, S.U.D.; Rana, U.A.; Andleeb, H.; Chopra, D.; Hameed, S.; Simpson, J. Exploiting the Role of Molecular Electrostatic Potential, Deformation Density, Topology, and Energetics in the Characterization of S···N and Cl···N Supramolecular Motifs in Crystalline Triazolothiadiazoles. *Cryst. Growth Des.* **2016**, *16*, 1371–1386. [CrossRef]
56. Valkonen, J.; Pitkanen, I.; Pajunen, A. Molecular and crystal structure and IR spectrum of 3,5-dibromo-1,2,4-triazole. *Acta Chem. Scand.* **1985**, *39*, 711–716. [CrossRef]

57. Berski, S.; Ciunik, Z.; Drabent, K.; Latajka, Z.; Panek, J. Dominant role of C–Br···N halogen bond in molecular self-organization. Crystallographic and quantum-chemical study of Schiff-base-containing triazoles. *J. Phys. Chem. B* **2004**, *108*, 12327–12332. [CrossRef]
58. Gilandoust, M.; Harsha, K.B.; Madan Kumar, S.; Rakesh, K.S.; Lokanath, N.K.; Byrappa, K.; Rangappa, K.S. 5-Bromo-1,2,4-triazolo[1,5-a]pyrimidine. *IUCrData* **2016**, *1*, x161944. [CrossRef]
59. Eccles, K.S.; Morrison, R.E.; Sinha, A.S.; Maguire, A.R.; Lawrence, S.E. Investigating C=S···I Halogen Bonding for Cocrystallization with Primary Thioamides. *Cryst. Growth Des.* **2015**, *15*, 3442–3451. [CrossRef]
60. Eliseeva, A.A.; Ivanov, D.M.; Novikov, A.S.; Kukushkin, V.Y. Recognition of the π-hole donor ability of iodopentafluorobenzene—A conventional σ-hole donor for crystal engineering involving halogen bonding. *CrystEngComm* **2019**, *21*, 616–628. [CrossRef]
61. Mochida, T.; Miura, Y.; Shimizu, F. Assembled Structures and Cation-Anion Interactions in Crystals of Alkylimidazolium and Alkyltriazolium Iodides with Ferrocenyl Substituents. *Cryst. Growth Des.* **2011**, *11*, 262–268. [CrossRef]
62. Guino-o, M.A.; Talbot, M.O.; Snits, M.M.; Pham, T.N.; Audi, M.C.; Janzen, D.E. Crystal structures of five 1-alkyl-4-aryl-1,2,4-triazol-1-ium halide salts. *Acta Cryst. E* **2015**, *71*, 628–635. [CrossRef]
63. Zhang, W.Y.; Yuan, J.Y. Poly(1-Vinyl-1,2,4-triazolium) Poly(Ionic Liquid)s: Synthesis and the Unique Behavior in Loading Metal Ions. *Macromol. Rapid Commun.* **2016**, *37*, 1124–1129. [CrossRef]
64. Gao, Y.; Twamley, B.; Shreeve, J.M. The first (ferrocenylmethyl)imidazollum and (ferrocenylmethyl)triazolium room temperature ionic liquids. *Inorg. Chem.* **2004**, *43*, 3406–3412. [CrossRef]
65. Darwich, C.; Karaghiosoff, K.; Klapotke, T.M.; Sabate, C.M. Synthesis and characterization of 3,4,5-Triamino-1,2,4-triazolium and 1-Methyl-3,4,5-triamino-1,2,4-triazolium iodides. *Z. Anorg. Allg. Chem.* **2008**, *634*, 61–68. [CrossRef]
66. McCrary, P.D.; Chatel, G.; Alaniz, S.A.; Cojocaru, O.A.; Beasley, P.A.; Flores, L.A.; Kelley, S.P.; Barber, P.S.; Rogers, R.D. Evaluating Ionic Liquids as Hypergolic Fuels: Exploring Reactivity from Molecular Structure. *Energy Fuels* **2014**, *28*, 3460–3473. [CrossRef]
67. Elnajjar, F.O.; Binder, J.F.; Kosnik, S.C.; Macdonald, C.L.B. 1,2,4-Triazol-5-ylidenes versus Imidazol-2-ylidenes for the Stabilization of Phosphorus(I) Cations. *Z. Anorg. Allg. Chem.* **2016**, *642*, 1251–1258. [CrossRef]
68. Talbot, M.O.; Pham, T.N.; Guino-o, M.A.; Guzei, I.A.; Vinokur, A.I.; Young, V.G. Investigation of ligand steric effect on the hydrogen gas produced via a nickel-catalyzed dehydrogenation of ammonia-borane utilizing unsymmetrical triazolylidene ligands. *Polyhedron* **2016**, *114*, 415–421. [CrossRef]
69. Ghazal, B.; Machacek, M.; Shalaby, M.A.; Novakova, V.; Zimcik, P.; Makhseed, S. Phthalocyanines and Tetrapyrazinoporphyrazines with Two Cationic Donuts: High Photodynamic Activity as a Result of Rigid Spatial Arrangement of Peripheral Substituents. *J. Med. Chem.* **2017**, *60*, 6060–6076. [CrossRef]
70. Zhang, H.; Wang, Z.Q.; Ghiviriga, I.; Pillai, G.G.; Jabeen, F.; Arami, J.A.; Zhou, W.F.; Steel, P.J.; Hall, C.D.; Katritzky, A.R. Synthesis, characterization and energetic properties of novel 1-methyl-1,2,4-triazolium N-aryl/N-pyridinyl ylids. *Tetrahedron Lett.* **2017**, *58*, 1079–1085. [CrossRef]
71. Yan, H.R.; Wang, J.; Yu, Y.H.; Hou, G.F.; Zhang, H.X.; Gao, J.S. Two cationic $[(Cu_xI_y)^{x-y}]_n$ motif based coordination polymers and their photocatalytic properties. *RSC Adv.* **2016**, *6*, 71206–71213. [CrossRef]
72. Jiang, Y.L.; Wang, Y.L.; Lin, J.X.; Liu, Q.Y.; Lu, Z.H.; Zhang, N.; Jia Jia, W.; Li, L.Q. Syntheses, structures and properties of coordination polymers of cadmium(II) with 4-methyl-1,2,4-triazole-3-thiol ligand. *CrystEngComm* **2011**, *13*, 1697–1706. [CrossRef]
73. Li, B.Y.; Peng, Y.; Li, G.H.; Hua, J.; Yu, Y.; Jin, D.; Shi, Z.; Feng, S.H. Design and Construction of Coordination Polymers by 4-Amino-3,5-bis(*n*-pyridyl)-1,2,4-triazole (n = 2, 3, 4) Isomers in a Copper(I) Halide System: Diverse Structures Tuned by Isomeric and Anion Effects. *Cryst. Growth Des.* **2010**, *10*, 2192–2201. [CrossRef]
74. Kuttatheyil, A.V.; Handke, M.; Bergmann, J.; Lassig, D.; Lincke, J.; Haase, J.; Bertmer, M.; Krautscheid, H. ^{113}Cd Solid-State NMR for Probing the Coordination Sphere in Metal-Organic Frameworks. *Chem. Eur. J.* **2015**, *21*, 1118–1124. [CrossRef]
75. Wang, X.; Guo, W.; Guo, Y.M. Controllable assemblies of Cd(II) supramolecular coordination complexes based on a versatile tripyridyltriazole ligand and halide/pseduohalide anions. *J. Mol. Struct.* **2015**, *1096*, 136–141. [CrossRef]
76. Yan, J.Z.; Lu, L.P. Syntheses, Crystal Structures and Luminescence Properties of Two Cu_4I_4 Coordination Polymers Based on 3,5-Dialkyl-1,2,4-triazole. *Chinese J. Inorg. Chem.* **2017**, *33*, 1697–1704. [CrossRef]

77. Tan, T.T.Y.; Schick, S.; Hahn, F.E. Synthesis and Reactivity of Ir^{III} Complexes Bearing C-Metalated Pyrazolato Ligands. *Organometallics* **2019**, *38*, 567–574. [CrossRef]
78. Libnow, S.; Wille, S.; Christiansen, A.; Hein, M.; Reinke, H.; Kockerling, M.; Miethchen, R. Synthesis and reactivity of halogenated 1,2,4-triazole nucleoside analogues with high potential for chemical modifications. *Synth.-Stuttg.* **2006**, *2006*, 496–508. [CrossRef]
79. Novikov, A.S.; Ivanov, D.M.; Bikbaeva, Z.M.; Bokach, N.A.; Kukushkin, V.Y. Noncovalent Interactions Involving Iodofluorobenzenes: The Interplay of Halogen Bonding and Weak Ip(O)$\cdots\pi$-$Hole_{(arene)}$ Interactions. *Cryst. Growth Des.* **2018**, *18*, 7641–7654. [CrossRef]
80. Bikbaeva, Z.M.; Ivanov, D.M.; Novikov, A.S.; Ananyev, I.V.; Bokach, N.A.; Kukushkin, V.Y. Electrophilic-Nucleophilic Dualism of Nickel(II) toward Ni$\cdots$I Noncovalent Interactions: Semicoordination of Iodine Centers via Electron Belt and Halogen Bonding via σ-Hole. *Inorg. Chem.* **2017**, *56*, 13562–13578. [CrossRef]
81. Bikbaeva, Z.M.; Novikov, A.S.; Suslonov, V.V.; Bokach, N.A.; Kukushkin, V.Y. Metal-mediated reactions between dialkylcyanamides and acetamidoxime generate unusual (nitrosoguanidinate)nickel(II) complexes. *Dalton Trans.* **2017**, *46*, 10090–10101. [CrossRef]
82. Andrusenko, E.V.; Kabin, E.V.; Novikov, A.S.; Bokach, N.A.; Starova, G.L.; Kukushkin, V.Y. Metal-mediated generation of triazapentadienate-terminated di- and trinuclear μ^2-pyrazolate Ni^{II} species and control of their nuclearity. *New J. Chem.* **2017**, *41*, 316–325. [CrossRef]
83. Mikherdov, A.S.; Novikov, A.S.; Kinzhalov, M.A.; Boyarskiy, V.P.; Starova, G.L.; Ivanov, A.Y.; Kukushkin, V.Y. Halides Held by Bifurcated Chalcogen–Hydrogen Bonds. Effect of $\mu_{(S,N-H)}$Cl Contacts on Dimerization of Cl(carbene)Pd^{II} Species. *Inorg. Chem.* **2018**, *57*, 3420–3433. [CrossRef]
84. Mikherdov, A.S.; Kinzhalov, M.A.; Novikov, A.S.; Boyarskiy, V.P.; Boyarskaya, I.A.; Avdontceva, M.S.; Kukushkin, V.Y. Ligation-Enhanced π-Hole$\cdots\pi$ Interactions Involving Isocyanides: Effect of π-Hole$\cdots\pi$ Noncovalent Bonding on Conformational Stabilization of Acyclic Diaminocarbene Ligands. *Inorg. Chem.* **2018**, *57*, 6722–6733. [CrossRef] [PubMed]
85. Adonin, S.A.; Bondarenko, M.A.; Novikov, A.S.; Abramov, P.A.; Sokolov, M.; Fedin, V.P. Halogen bonding in the structures of pentaiodobenzoic acid and its salts. *CrystEngComm* **2019**, *21*, 6666–6670. [CrossRef]
86. Afanasenko, A.M.; Novikov, A.S.; Chulkova, T.G.; Grigoriev, Y.M.; Kolesnikov, I.E.; Selivanov, S.I.; Starova, G.L.; Zolotarev, A.A.; Vereshchagin, A.N.; Elinson, M.N. Intermolecular interactions-photophysical properties relationships in phenanthrene-9,10-dicarbonitrile assemblies. *J. Mol. Struct.* **2020**, *1199*, 126789. [CrossRef]
87. Yandanova, E.S.; Ivanov, D.M.; Kuznetsov, M.L.; Starikov, A.G.; Starova, G.L.; Kukushkin, V.Y. Recognition of S$\cdots$CI Chalcogen Bonding in Metal-Bound Alkylthiocyanates. *Cryst. Growth Des.* **2016**, *16*, 2979–2987. [CrossRef]
88. Bulatova, M.; Melekhova, A.A.; Novikov, A.S.; Ivanov, D.M.; Bokach, N.A. Redox reactive (RNC)Cu^{II} species stabilized in the solid state via halogen bond with I_2. *Z. Kristallogr. Cryst. Mater.* **2018**, *233*, 371–377. [CrossRef]
89. Rozhkov, A.V.; Novikov, A.S.; Ivanov, D.M.; Bolotin, D.S.; Bokach, N.A.; Kukushkin, V.Y. Structure-Directing Weak Interactions with 1,4-Diiodotetrafluorobenzene Convert One-Dimensional Arrays of $[M^{II}(acac)_2]$ Species into Three-Dimensional Networks. *Cryst. Growth Des.* **2018**, *18*, 3626–3636. [CrossRef]
90. Kinzhalov, M.A.; Kashina, M.V.; Mikherdov, A.S.; Mozheeva, E.A.; Novikov, A.S.; Smirnov, A.S.; Ivanov, D.M.; Kryukova, M.A.; Ivanov, A.Y.; Smirnov, S.N.; et al. Dramatically Enhanced Solubility of Halide-Containing Organometallic Species in Diiodomethane: The Role of Solvent$\cdots$Complex Halogen Bonding. *Angew. Chem. Int. Ed.* **2018**, *57*, 12785–12789. [CrossRef]
91. Zelenkov, L.E.; Ivanov, D.M.; Avdontceva, M.S.; Novikov, A.S.; Bokach, N.A. Tetrachloromethane as halogen bond donor toward metal-bound halides. *Z. Kristallogr. Cryst. Mater.* **2019**, *234*, 9–17. [CrossRef]
92. Baykov, S.V.; Dabranskaya, U.; Ivanov, D.M.; Novikov, A.S.; Boyarskiy, V.P. Pt/Pd and I/Br Isostructural Exchange Provides Formation of C–I$\cdots$Pd, C–Br$\cdots$Pt, and C–Br$\cdots$Pd Metal-Involving Halogen Bonding. *Cryst. Growth Des.* **2018**, *18*, 5973–5980. [CrossRef]
93. Espinosa, E.; Molins, E.; Lecomte, C. Hydrogen bond strengths revealed by topological analyses of experimentally observed electron densities. *Chem. Phys. Lett.* **1998**, *285*, 170–173. [CrossRef]

94. Vener, M.V.; Egorova, A.N.; Churakov, A.V.; Tsirelson, V.G. Intermolecular hydrogen bond energies in crystals evaluated using electron density properties: DFT computations with periodic boundary conditions. *J. Comput. Chem.* **2012**, *33*, 2303–2309. [CrossRef] [PubMed]
95. Bartashevich, E.V.; Tsirelson, V.G. Interplay between non-covalent interactions in complexes and crystals with halogen bonds. *Russ. Chem. Rev.* **2014**, *83*, 1181–1203. [CrossRef]
96. Espinosa, E.; Alkorta, I.; Elguero, J.; Molins, E. From weak to strong interactions: A comprehensive analysis of the topological and energetic properties of the electron density distribution involving X–H···F–Y systems. *J. Chem. Phys.* **2002**, *117*, 5529–5542. [CrossRef]